29 May 1998

ELSEVIER

Chemical Physics Letters 288 (1998) 621–627

CHEMICAL PHYSICS LETTERS

A direct dynamics study of the $F + C_2H_4 \rightarrow C_2H_3F + H$ product energy distributions

Kim Bolton [a], William L. Hase [a], H. Bernhard Schlegel [a], Kihyung Song [b]

[a] *Department of Chemistry, Wayne State University, Detroit, MI 48202, USA*
[b] *Department of Chemistry, Korea Nat'l University of Education, Chongwon, Chungbuk 363-791, South Korea*

Received 18 December 1997

Abstract

Ab initio direct dynamics was used to calculate product energy distributions for the $F + C_2H_4 \rightarrow C_2H_3F + H$ reaction. A broad product translational energy distribution, similar to that observed experimentally, is found when the trajectories are initialized with a statistical vibrational energy distribution at the exit channel barrier. The trajectories show that, on average, orbital angular momentum is conserved in going from the exit channel barrier to products, and a model which incorporates this dynamical constraint reproduces the ensemble averaged trajectory results.

1. Introduction

An explanation of the product energy distributions measured [1,2] for the reaction

$$F + C_2H_4 \rightarrow C_2H_3F + H \qquad (R1)$$

remains an important issue [1–10] in unimolecular rate theory. Crossed molecular beam experiments [1,2] with a reactant relative translational energy E_{rel} of 2 to 12 kcal mol^{-1}, indicate that the product relative translational energy E'_{rel} distribution is broad, with an average value of $\approx 50\%$ of the total available energy. Infrared chemiluminescence experiments [3] show that the C_2H_3F product is formed with a nonstatistical vibrational energy distribution. These results are not in accord with a simple model which assumes a statistical distribution of energy at the $C_2H_3F \cdots H^{\ddagger}$ transition state, as predicted by RRKM theory, followed by repulsive energy release in which all the exit channel potential goes to product relative translation. To reconcile theory and experiment, more detailed models [4–8] have been advanced for understanding the product energy partitioning. Though these studies provided more insight into the dynamics of the Reaction (R1) product energy partitioning, they have not given quantitative interpretations of the experimental results.

One of these previous studies [8] was a classical trajectory simulation based on an analytic potential energy surface (PES) derived in part from UHF/4-31G calculations. Subsequent higher level ab initio calculations [9,10] have identified shortcomings of this analytic PES, which may affect the product energy partitioning. Thus, there is an interest in performing an additional trajectory study with a more accurate PES.

An attractive trajectory approach is 'direct dynamics' [11], in which trajectories are integrated 'on the fly', using forces and second-order derivatives (when required) obtained directly from an electronic structure theory at each integration step. However, such a

0009-2614/98/$19.00
PII: S0009-2614(98)00274-7

calculation is computationally expensive and there is a limit on the level of electronic structure theory which may be used. Fortunately, the UHF/6-31G* level of theory, which is tractable for direct dynamics, gives stationary point, geometries and normal mode frequencies and exit channel energetics for Reaction (R1) similar to those determined at higher levels of theory, e.g., QCISD/6-311G** [1]. In the work presented here UHF/6-31G* direct dynamics is used to study product energy partitioning for Reaction (R1) and for the reaction

$$H + C_2H_4 \rightarrow C_2H_4 + H \qquad (R2)$$

so that the dynamics for Reactions (R1) and (R2) may be compared.

The trajectories are initialized at the exit channel barrier for each of these reactions, for both practical and fundamental reasons. First, it is computationally prohibitive to use ab initio direct dynamics to simulate the complete reaction and calculate a sufficient number of events. Second, even if this could be done (e.g., by semiempirical direct dynamics [11]) it would not be the best way to use direct dynamics to calculate the product energy distributions. By initializing the trajectories at the exit channel barrier, quasiclassical conditions [12] with the correct zero point energy may be assured at the barrier. In addition, comparisons between classical and quantum dynamics have shown [13] that classical dynamics gives accurate results for a direct process like the motion down a potential energy barrier, if the trajectories are initialized with the correct quasiclassical conditions. Thus, if the correct initial ensemble of states is chosen at the barrier and the exit channel potential is correct, agreement between classical trajectory and experimental results is expected.

For rovibrationally cold reactants, the conditions in the crossed molecular beam experiments for Reaction (R1), the energy available to the products E' may be expressed as

$$E' = E_{rel} - \Delta H_0^0 \qquad (1)$$

where E_{rel} is the reactant relative translational energy and ΔH_0^0 is the 0 K heat of reaction. The experimental 300 K heats of formation [14] for C_2H_3F (-33.2 kcal mol^{-1}), C_2H_4 (12.5 kcal mol^{-1}), H (52.1 kcal mol^{-1}) and F (19.0 kcal mol^{-1}) and experimental anharmonic frequencies for C_2H_3F and C_2H_4 give [15] $\Delta H_0^0 = -12.8$ kcal mol^{-1} for Reaction (R1), which is similar to the values of -11 [1], -14 [2] and -15 ± 2 [10] assumed previously. E' may also be expressed as

$$E' = E^{\ddagger} + E_0 \qquad (2)$$

where $E^{\ddagger}$ is the energy at the exit channel barrier in excess of the zero point energy and E_0 is the exit channel barrier height with zero point energies included.

2. UHF/6-31G* potential energy surface

The C_2H_4 and C_2H_3F minimum energy geometries obtained at the UHF/6-31G* level of theory are planar and in very good agreement with experiment [16,17]. The UHF/6-31G* geometries for the $C_2H_4 \cdots H^{\ddagger}$ and $C_2H_3F \cdots H^{\ddagger}$ transition states are in good agreement with those determined at higher levels of theory [18].

The height of the exit channel barriers for Reactions (R1) and (R2) have not been converged by ab initio calculations [10,18]. The UHF/6-31G* exit channel barrier height, E_0, for Reactions (R1) and (R2), with zero point energies included, are 6.39 and 3.11 kcal mol^{-1}, respectively. Using ab initio structures and vibrational frequencies to fit the H + $C_2H_4 \rightarrow C_2H_5$ experimental rate constant, $E_0 =$ 2.70 kcal mol^{-1} has been deduced for Reaction (R2) [19], in good agreement with the UHF/6-31G* value. Since the H + $C_2H_3F \rightarrow C_2H_4F$ association rate has not been measured, the above approach cannot be used to deduce a value of E_0 for this reaction. However, ab initio and experimental data were used to estimate a value of 5–6 kcal mol^{-1} for this E_0 [10], in agreement with the UHF/6-31G* value.

At the UHF/6-31G* level of theory, the two transitional bending mode frequencies are 414 and 446 cm^{-1} for $C_2H_4 \cdots H^{\ddagger}$ and 456 and 480 cm^{-1} for $C_2H_3F \cdots H^{\ddagger}$. The QCISD/6-311G** and MRCI/cc-pVDZ higher levels of theory give transitional mode frequencies for $C_2H_4 \cdots H^{\ddagger}$ which are

[1] To be discussed in a subsequent paper.

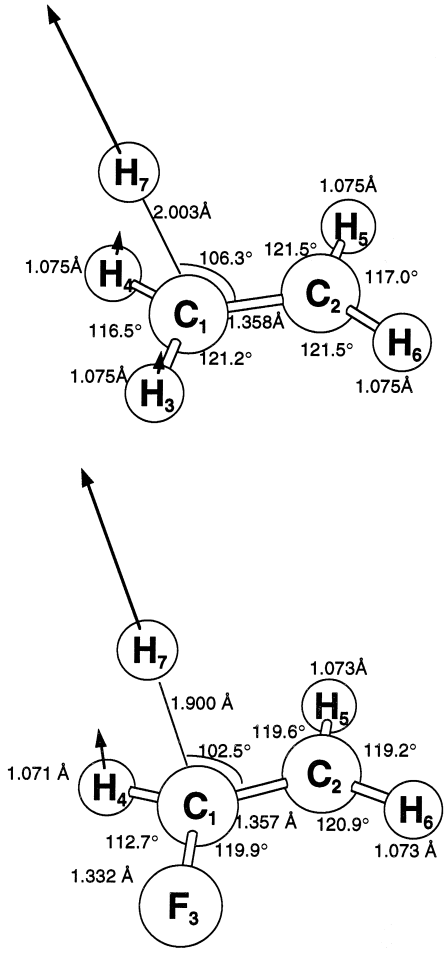

Fig. 1. $C_2H_4 \cdots H^{\ddagger}$ and $C_2H_3F \cdots H^{\ddagger}$ transition structures obtained at the UHF/6-31G* level of theory [9]. The out-of-plane wag angles are: $C_2C_1H_3H_4 = 169.7°$ and $C_1C_2H_5H_6 = 177.4°$ for the $C_2H_4 \cdots H^{\ddagger}$ structure, and $C_2C_1F_3H_4 = 164.8°$ and $C_1C_2H_5H_6 = 175.6°$ for the fluorinated structure. The reaction coordinate eigenvectors are superimposed on these structures.

only ten and two percent different than the UHF/6-31G* values, respectively [18]. Fig. 1 shows that the UHF/6-31G* reaction coordinate eigenvectors for both $C_2H_4 \cdots H^{\ddagger}$ and $C_2H_3F \cdots H^{\ddagger}$ include H–C $\cdots$ H angle bending motion. The same property is found at the higher level of theories (see footnote 1).

3. Direct dynamics method

Ensembles of trajectories with total energies $E^{\ddagger}$ of 14, 19 and 24 kcal mol^{-1} were initialized at the exit channel barriers for Reactions (R1) and (R2) and propagated towards products. From Eqs. (1) and (2), these $E^{\ddagger}$ values correspond to E_{rel} of ≈ 8, 13 and 18 kcal mol^{-1} for Reaction (R1), which are in the range of E_{rel} values studied experimentally (2–12 kcal mol^{-1}) and in the classical trajectory simulation (20 kcal mol^{-1}).

The RRKM assumption [20,21] that vibrational energy levels of the transition state have equal probabilities of being populated, is used to choose initial conditions for the trajectories. The total angular momentum $\boldsymbol{J}$ and its components $J_x^{\ddagger}$, $J_y^{\ddagger}$ and $J_z^{\ddagger}$ in the principal rotational axes frame of the transition state were chosen from distributions appropriate for the molecular beam experiments. These distributions were determined by running trajectories on the analytic PES for the complete $F + C_2H_4 \rightarrow C_2H_3F + H$ reaction and halting the trajectories at the exit channel barrier (specified by the $C_2H_3F \cdots H^{\ddagger}$ distance $r_{HC}^{\ddagger} = 1.95$ Å). The $C_2H_3F \cdots H^{\ddagger}$ moiety was then rotated into its principal axis frame to find $J_x^{\ddagger}$, $J_y^{\ddagger}$ and $J_z^{\ddagger}$.

The total angular momentum $\boldsymbol{J}$ distribution is quite broad, as found in the previous trajectory study, i.e., Fig. 3c of Ref. [8]. For a $F + C_2H_4$ E_{rel} of 13.0 kcal mol^{-1}, i.e., $E^{\ddagger} = 19$ kcal mol^{-1} for the UHF/6-31G* PES, the J distribution is peaked at approximately 40 $\hbar$ with an average of 52.3 $\hbar$. The distributions of $J_x^{\ddagger}$, $J_y^{\ddagger}$ and $J_z^{\ddagger}$ for this J distribution are shown in Fig. 2 ($J_x^{\ddagger}$ is the component of J that

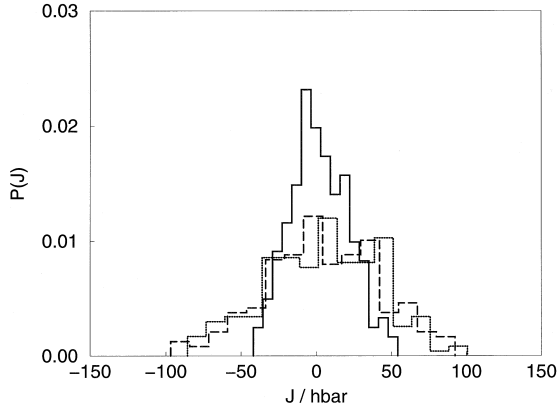

Fig. 2. Distributions of $J_x^{\ddagger}$ (solid line), $J_y^{\ddagger}$ (dashed line) and $J_z^{\ddagger}$ (dotted line) at the $C_2H_3F \cdots H^{\ddagger}$ transition state for the $F + C_2H_4 \rightarrow C_2H_3F + H$ trajectories run on the analytic PES with $E_{rel} = 13.0$ kcal mol^{-1}. $J_z^{\ddagger}$ is the component of $\boldsymbol{J}$ perpendicular to the F–C–C plane and $J_x^{\ddagger}$ is the component lying approximately along the F–C–C axis.

approximately lies along the F–C–C axis and $J_z^{\ddagger}$ the component perpendicular to the F–C–C plane). The average values of the magnitudes of the distributions are $\langle J_x^{\ddagger}\rangle = 15.6\,\hbar$, $\langle J_y^{\ddagger}\rangle = 30.4\,\hbar$ and $\langle J_z^{\ddagger}\rangle = 31.1\,\hbar$. It is interesting to note that the similar values for $\langle J_y^{\ddagger}\rangle$ and $\langle J_z^{\ddagger}\rangle$ and the finding that the probabilities for all three components peak at zero $\hbar$ (consistent with a random projection of J [22]) do not support the kinematic model proposed by Lee and coworkers in which the F atom adds perpendicular to the C_2H_4 plane with $\boldsymbol{J} \approx J_y^{\ddagger} \approx \boldsymbol{j}'$, where $\boldsymbol{j}'$ is the C_2H_3F rotational angular momentum [2].

Quasiclassical rigid rotor/normal mode sampling [12,23] was used to select initial conditions for the UHF/6-31G* direct dynamics trajectories by: (1) selecting J and its components from the above distributions and calculating the transition state rotational energy from

$$E_{\mathrm{rot}}^{\ddagger} = \sum_{i=x,y,z} \left(J_i^{\ddagger}\right)^2 / 2I_i^{\ddagger} \tag{3}$$

where the $I_i^{\ddagger}$ are the transition state's principal moments of inertia; (2) randomly selecting a transition state normal mode vibrational energy level in the range 0–$E_{\mathrm{int}}^{\ddagger}$ [23], where

$$E_{\mathrm{int}}^{\ddagger} = E^{\ddagger} - E_{\mathrm{rot}}^{\ddagger}; \tag{4}$$

and (3) transforming the normal mode energies to Cartesian coordinates and momenta [24,25].

The trajectories were propagated by integrating Newton's equations of motion either in Cartesian coordinates and momenta using the Gauss-Radau algorithm [26–28], or by integrating the instantaneous normal modes [29–31]. The relative merits of these techniques will be discussed elsewhere [32]. Trajectories were integrated until the force between the product fragments was less than 10^{-4} kcal mol^{-1} Å^{-1}. Trajectories were typically 50 to 100 fs, and the products were separated by 5.5–6.0 Å. A typical trajectory for Reaction (R2) was integrated in ≈ 176 min on an IBM RS6000/560.

[2] The relative velocity scattering angle distribution $\theta(v,v')$ reported in Ref. [8] was not normalized by $\sin\theta$ and supports the distributions of $\boldsymbol{J}$ components found here and not the model of Lee and coworkers as deduced previously.

Properties that were monitored are product relative translational, rotational and vibrational energies, E'_{rel}, E'_{rot} and E'_{vib}; the orbital $\boldsymbol{l}$ and C_2H_3F (or C_2H_4) rotational angular momentum $\boldsymbol{j}$ at the transition state and for the products; the fragment's relative translational energy $E_{\mathrm{rel}}^{\ddagger}$ at the transition state; the centrifugal potential at the transition state,

$$V_{\mathrm{cen}}^{\ddagger} = \frac{\left(\boldsymbol{l}^{\ddagger}\right)^2}{2\mu\left(r^{\ddagger}\right)^2} \tag{5}$$

where $\boldsymbol{l}^{\ddagger}$ is the fragments' orbital angular momentum, μ their reduced mass and $r^{\ddagger}$ their center of mass distance; and the sum

$$E_{\mathrm{rel}}^{\mathrm{iso}} = E_{\mathrm{rel}}^{\ddagger} + V_{\mathrm{cen}}^{\ddagger} + E_0 \tag{6}$$

which would be the product relative translational energy for an isotropic exit channel potential.

4. Results and discussion

Ensembles of 140–160 trajectories were calculated for Reactions (R1) and (R2), with different conditions for $E^{\ddagger}$ and J. The results are listed in Table 1. The entry in the fifth row of the table is for a calculation in which the forces are for the C_2H_5 PES, but with the mass of one of the ethylenic H atoms of the $H\cdots CH_2$ moiety changed to the mass of a F atom to model the kinematics of the $C_2H_3F\cdots H^{\ddagger} \rightarrow C_2H_3F + H$ reaction. The average fraction $\langle f'_{\mathrm{rel}}\rangle$ of the available energy that goes to E'_{rel} is slightly larger for Reaction (R1) than for Reaction (R2). Within statistical uncertainty, $\langle f'_{\mathrm{rel}}\rangle$ is the same for $J = 0$ and the simulations with a $\boldsymbol{J}$ distribution to model the beam experiments, and is also insensitive to substituting the mass of an ethylene H atom by the F mass. The value of $\langle f'_{\mathrm{rel}}\rangle = 0.50$ found here for Reaction (R1) is larger than the 0.32 found from the previous trajectory study.

The same angular momentum constraints observed in the previous trajectory study are found in this direct dynamics simulation. The system's total angular momentum J is primarily converted to product (C_2H_4 or C_2H_3F) rotational angular momentum j'. This correlation explains why $\langle f'_{\mathrm{rot}}\rangle$ significantly increases for the $C_2H_4\cdots H^{\ddagger} \rightarrow C_2H_4 + H$ simulation when $\boldsymbol{J}$ changes from zero to a distribution

Table 1
Ensemble averages at the exit channel barrier and for the products [a]

Initial conditions		Transition state				Products					
$E^{\ddagger}$	J	$E^{\ddagger}_{rel}$	E^{iso}_{rel}	$l^{\ddagger}$	$j^{\ddagger}$	E'	f'_{rel}	f'_{rot}	f'_{vib}	l'	j'
		$C_2H_4 \cdots H^{\ddagger} \rightarrow C_2H_4 + H$									
14.0	0	2.3	6.3	8.8	8.8	17.11	0.38	0.03	0.59	9.1	9.1
19.0	0	2.4	7.6	14.0	14.0	22.11	0.39	0.05	0.56	14.0	14.0
24.0	0	3.0	8.5	14.3	14.3	27.11	0.37	0.05	0.58	14.8	14.8
19.0	beam [b]	2.5	9.1	17.2	48.4	22.11	0.42	0.38	0.20	18.3	48.1
19.0	beam [b,c]	2.2	8.4	15.8	51.1	22.11	0.38	0.23	0.39	15.6	51.2
		$C_2H_3F \cdots H^{\ddagger} \rightarrow C_2H_3F + H$									
19.0	beam [b]	2.8	12.4	15.7	54.2	25.39	0.50	0.18	0.32	16.8	55.0

[a] Energy is in kcal mol^{-1} and angular momentum in units of $\hbar$. The standard deviation in the average $E^{\ddagger}_{rel}$, f'_{rot} and f'_{vib} is $\approx 6\%$, and in E^{iso}_{rel}, f'_{rel}, $l^{\ddagger}$, $j^{\ddagger}$, l' and j' is $\approx 3\%$. [b] The J distribution simulated for $F + C_2H_4 \rightarrow C_2H_3F \cdots H^{\ddagger}$ is shown in Fig. 2. [c] Forces determined from the C_2H_5 surface, but propagation performed using masses appropriate to the fluorinated reaction (see text).

representing the molecular beam experiments. The ensemble averaged orbital angular momentum is conserved quite well when proceeding from the transition state to the products. This is illustrated by the similarity of the $\langle l^{\ddagger} \rangle$ and $\langle l' \rangle$ values in Table 1. The correlation coefficients for $(l^{\ddagger},l')$, which provide a measure of the orbital angular momentum conservation over individual trajectories, range from 0.75 to 0.99 for the conditions shown in Table 1. Substituting the fluorine mass for the hydrogen mass increases the $(l^{\ddagger},l')$ correlation, and integration on the C_2H_4F PES instead of the C_2H_5 PES decreases the correlation.

Because of the conservation of $\langle l \rangle$ in the exit channel, the centrifugal potential at the transition state, Eq. (5), is, on the average, converted to product relative translational energy. Furthermore, a model that assumes the exit channel channel barrier potential is transferred to product translation, Eq. (6), gives a good representation of the E'_{rel} averages. The only differences between $\langle E^{iso}_{rel} \rangle$ and $\langle E'_{rel} \rangle$ larger than 0.3 kcal mol^{-1} are for the $J = 0$ $C_2H_4 \cdots H^{\ddagger}$ calculations with $E^{\ddagger}$ of 19.0 and 24.0 kcal mol^{-1}. This correlation between E^{iso}_{rel} and E'_{rel} is only mildly retained for individual trajectories. For Reaction (R2), the $(E^{iso}_{rel}, E'_{rel})$ correlation coefficient varies from 0.76 at $E^{\ddagger} = 24$ kcal mol^{-1}, $J = 0$, to 0.84 at $E^{\ddagger} =$ 19 kcal mol^{-1} with J representing the beam simulations. For Reaction (R1) at $E^{\ddagger} = 19$ kcal mol^{-1} and J representing the beam simulations, the $(E^{iso}_{rel}, E'_{rel})$ correlation coefficient is just 0.69.

Distributions of E'_{rel} and E^{iso}_{rel} are compared in Fig. 3 for Reaction (R2) with $E^{\ddagger} = 19$ kcal mol^{-1}. The E^{iso}_{rel} distribution gives a good overall representation of the product relative translational energy distribution $P(E'_{rel})$. Choosing J to represent the beam simulation instead of setting it to zero has the effect of broadening, but not significantly shifting, the distribution (see $\langle f'_{rel} \rangle$ in Table 1).

Comparison of the $P(E'_{rel})$ and $P(E^{iso}_{rel})$ for Reaction (R1) with $E^{\ddagger} = 19$ kcal mol^{-1} and with the J distribution representing the beam simulation is given in Fig. 4. (These conditions correspond to $E_{rel} = 12.6$

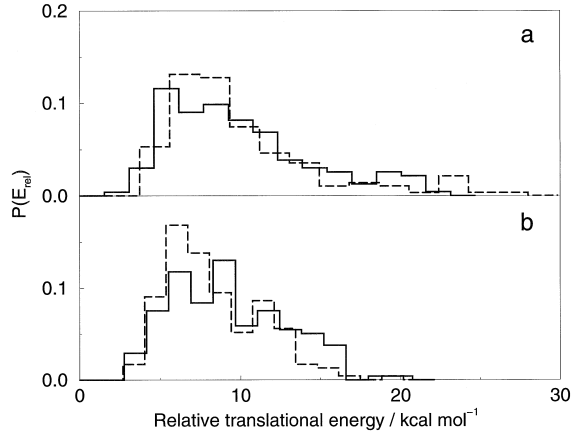

Fig. 3. Normalized direct dynamics distributions of E'_{rel} (solid line) and E^{iso}_{rel} (dashed line) for Reaction (R2) at $E^{\ddagger} = 19$ kcal mol^{-1}: (a) J is chosen from a distribution representing the molecular beam simulations and (b) $J = 0$.

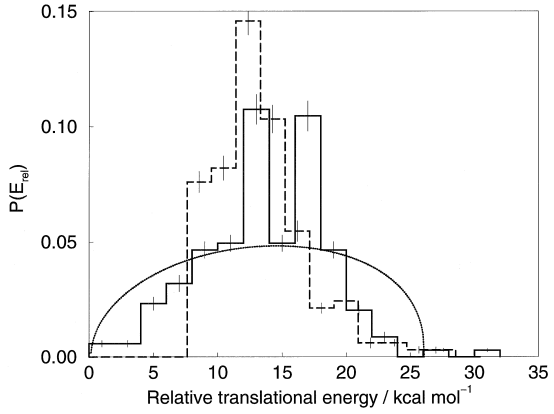

Fig. 4. Normalized distributions for Reaction (R1). Direct dynamics distributions at $E^{\ddagger} = 19$ kcal mol^{-1} (corresponding to $E_{rel} = 12.6$ kcal mol^{-1}) and $\boldsymbol{J}$ chosen from the molecular beam simulation, of E'_{rel} (solid line) and E^{iso}_{rel} (dashed line). E'_{rel} distribution deduced from experiment at $E_{rel} = 12.1$ kcal mol^{-1} (dotted line). Error bars, which reflect standard deviations, are shown by the vertical lines.

kcal mol^{-1}.) The E'_{rel} distribution is broader than the E^{iso}_{rel} distribution, but since the broadening is to both higher and lower energies, there is not a significant shift in the averages of the distributions. Also shown in Fig. 4 is the E'_{rel} distribution for $E_{rel} = 12.1$ kcal mol^{-1} deduced from the crossed molecular beam study of Reaction (R1) [2]. The UHF/6-31G* direct dynamics distribution has similar broadening as the experimental distribution, and the $\langle f'_{rel} \rangle$ of 0.5 obtained from the direct dynamics study is the same as the experimental value. The stronger peaking in the direct dynamics E'_{rel} distribution is probably not significant. To deduce the experimental $P(E'_{rel})$, a translation to a center of mass frame from the experimental laboratory frame was required. This transformation may be rather insensitive to peaking in $P(E'_{rel})$ as long as the distribution has the proper breadth. Also, in the experiment there is a small spread in the initial relative translational energy, which has the effect of removing structure, e.g. peaking, in the $P(E'_{rel})$ [33].

In summary, the following are the important results of the direct dynamics study of the $C_2H_3F \cdots H^{\ddagger} \rightarrow C_2H_3F + H$ exit channel dynamics.

1. As observed in the previous trajectory study of the complete reaction, angular momentum constraints are important. Overall rotational angular momentum is converted to C_2H_3F rotational angular momentum and orbital angular momentum is, on the average, conserved in proceeding from the exit channel transition state to the products. As a result of this latter constraint, the centrifugal potential at the transition state is converted to product relative translational energy.
2. A model based on isotropic exit channel dynamics which assumes the product relative translational distribution $P(E'_{rel})$ arises from the centrifugal potential and relative translational energy distributions at the transition state plus the exit channel potential release, gives very good agreement with the ensemble averaged trajectory results. However, this model is not valid for individual trajectories.
3. If a statistical population of vibrational energy levels at the exit channel transition state is assumed, and the angular momentum is chosen to represent the molecular beam experiment, the UHF/6-31G* direct dynamics E'_{rel} distribution is similar to the distribution deduced from crossed molecular beam experiments, and the average fraction of the available energy that goes to product translation is the same, i.e., 0.5.

Acknowledgements

K.B. and W.L.H. are grateful for financial support from the National Science Foundation, CHE-94-03780. H.B.S. is grateful for support from the same source, CHE-94-00678.

References

[1] J.M. Parson, Y.T. Lee, J. Chem. Phys. 56 (1972) 4658.
[2] J.M. Farrar, Y.T. Lee, J. Chem. Phys. 65 (1976) 1414.
[3] J.G. Moehlmann, J.T. Gleaves, J.W. Hudgens, J.D. McDonald, J. Chem. Phys. 60 (1974) 4790.
[4] R.A. Marcus, J. Chem. Phys. 62 (1975) 1372.
[5] G. Worry, R.A. Marcus, J. Chem. Phys. 67 (1977) 1636.
[6] D.J. Zvijac, S. Mukamel, J. Ross, J. Chem. Phys. 67 (1977) 2007.
[7] S. Kato, K. Morokuma, J. Chem. Phys. 72 (1980) 206.
[8] W.L. Hase, K.C. Bhalla, J. Chem. Phys. 75 (1981) 2807.
[9] H.B. Schlegel, J. Phys. Chem. 86 (1982) 4878.

[10] H.B. Schlegel, K.C. Bhalla, W.L. Hase, J. Phys. Chem. 86 (1982) 4883.
[11] K. Bolton, W.L. Hase, G.H. Peslherbe, in: D.L. Thompson (Ed.), Multidimensional Molecular Dynamics Methods, World Scientific, New Jersey, to appear.
[12] D.L. Bunker, Meth. Comput. Phys. 10 (1971) 287.
[13] A. Untch, R. Schinke, R. Cotting, J.R. Huber, J. Chem. Phys. 99 (1993) 9553.
[14] D.R. Lide (Ed.), CRC Handbook of Chemistry and Physics, Boca Raton, New York, 1997, 78th ed.
[15] D.A. McQuarrie, Statistical Mechanics, Harper Collins, New York, 1976.
[16] D.R. Lide Jr., D. Christensen, Spectrochim. Acta 17 (1961) 665.
[17] J.L. Duncan, I.J. Wright, D. Van Lerberghe, J. Mol. Spectrosc. 42 (1972) 463.
[18] W.L. Hase, H.B. Schlegel, V. Balbyshev, M. Page, J. Phys. Chem. 100 (1996) 5354.
[19] W.L. Hase, H.B. Schlegel, V. Balbyshev, M. Page, J. Phys. Chem. A 101 (1997) 5026.
[20] P.J. Robinson, K.A. Holbrook, Unimolecular Reactions, Wiley-Interscience, New York, 1972.
[21] W. Forst, Theory of Unimolecular Reactions, Academic Press, New York, 1973.
[22] D.L. Bunker, W.L. Hase, J. Chem. Phys. 59 (1973) 4621.
[23] C. Doubleday Jr., K. Bolton, G.H. Peslherbe, W.L. Hase, J. Am. Chem. Soc. 118 (1996) 9922.
[24] E.B. Wilson Jr., J.C. Decius, P.C. Cross, Molecular Vibrations, McGraw-Hill, New York, 1955.
[25] S. Chapman, D.L. Bunker, J. Chem. Phys. 62 (1975) 2890.
[26] E. Everhart, Celest. Mech. 10 (1974) 35.
[27] E. Everhart, in: A. Carusi, G.B. Valsecchi (Eds.), Dynamics of Comets: Their Origin and Evolution, Reidel, Dordrecht, 1985.
[28] K. Bolton, S. Nordholm, J. Comput. Phys. 113 (1994) 320.
[29] T. Helgaker, E. Uggerud, H. Jensen, Chem. Phys. Lett. 173 (1990) 145.
[30] E. Uggerud, T. Helgaker, J.Am. Chem. Soc. 114 (1992) 4266.
[31] W. Chen, W.L. Hase, H.B. Schlegel, Chem. Phys. Lett. 228 (1994) 436.
[32] K. Bolton, W.L. Hase, H.B. Schlegel, to be submitted.
[33] J.M. Parson, private communication.